International Conference on Computational Methods in Marine Engineering
MARINE 2005
P. Bergan , J. García, E. Oñate, and T. Kvamsdal, (Eds)

CALIBRATION OF A FATIGUE LIMIT STATE FOR MOORING LINES

Jan Mathisen*, Torfinn Hørte*
* Det Norske Veritas
N-1322 Høvik, Norway
e-mail: Jan.Mathisen@dnv.com, Torfinn.Horte@dnv.com, web page: http://www.dnv.com/

Key words: mooring lines, fatigue limit state, structural reliability, design code calibration.

Abstract. *A structural reliability method is applied to calibrate the safety factor of a fatigue design method for the mooring lines of floating offshore platforms. Both methods are based on the Miner Palmgren hypothesis for the accumulation of fatigue damage. The reliability analysis takes explicit account of the various uncertainties in the fatigue capacity, the damage accumulation and the calculation of mooring line tensions. These uncertainties are all intended to be covered by the safety factor in the design analysis. The uncertainty in the fatigue capacity is developed for chain and steel wire rope. A test set of six floating platforms in various water depths is considered. The effect of varying numbers of mooring line components is taken into account. A target probability of failure is established. The safety factor of the design method is calibrated to yield designs close to the target probability. This calibration is effected by minimising an objective function based on the difference between target probability and calculated probability of failure for the mooring lines in the test set. Under-design is penalised more heavily than over-design.*

1 INTRODUCTION

Offshore petroleum production has gradually been moving into deeper water, requiring floating platforms with longer and longer mooring lines. Det Norske Veritas and Marintek organised a joint industry project in 1996, to extend a design standard for positioning systems to deeper water. Structural reliability methods were systematically used to calibrate the design limit states. This implies that the design requirements are optimised such that they yield designs with the specified target reliability. Thus, the reliability level implied by each limit state is now quantified and the reliability of mooring lines designed to the standard can chosen to be consistent with the consequences of failure, and with the reliability of other components of the offshore production system. The calibration of the ultimate and accidental limit states has previously been published[1],[2]. The present paper describes the calibration of the fatigue limit state[3]. The results of the calibrations are incorporated in DNV's offshore standard for position mooring[4].

2 CALIBRATION METHOD

An overview of the calibration process is shown in Figure 1, based on the principles stated in ref. [5]. The process starts by defining the scope of the design code that is to be calibrated. A set of test structures is then chosen to span this scope, while limiting the size of the test set to avoid excessive computational effort in the calibration. The target reliability level for the

design code also has to be chosen. This can be a difficult choice, and will typically be preceded by some pilot reliability analyses. The initial format of the design criterion is then chosen and expressed as a design equation to provide the single missing parameter in the specification of each test design.

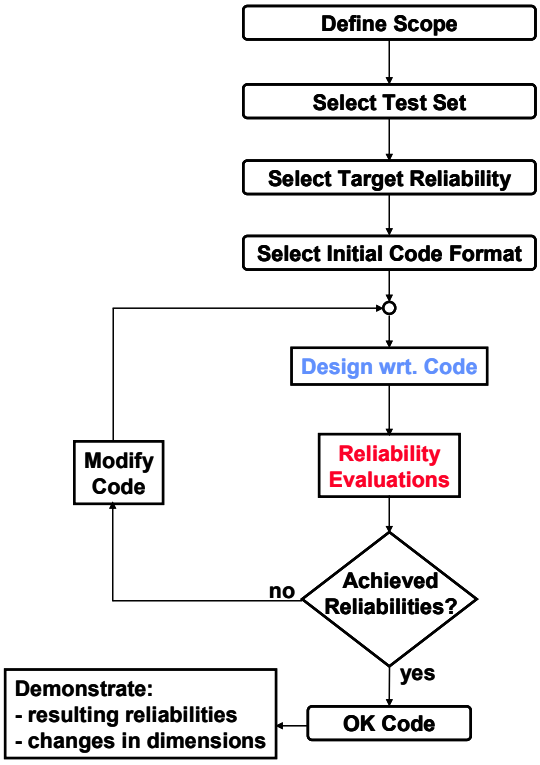

Figure 1: Overview of calibration process.

An iteration loop forms the main part of the process, in which the design code is adjusted in order to yield designs with the target reliability. Any aspect of the design code can be modified, but it is convenient to simply discuss modification of the fatigue safety factor γ. This factor is given a trial value at the start of the iteration. Each mooring system in the test set is designed to satisfy the design equation, using the assumed safety factor. The probability of failure $P_{Fi}[\gamma]$ is determined for each mooring system in the test set $i = 1,2,...,n$, and is effectively a function of the trial value of the safety factor γ. An objective function is applied to assess the distance of the obtained reliabilities from the target reliability. The objective function is formulated as

$$\Delta = \sum_{i=1}^{i=n} \left(P_{Fi}[\gamma] - P_T \right)^2 \qquad \textbf{(1)}$$

where P_T is the target probability of failure. The optimum safety factor is found by minimizing the value of this objective function. Note that this form of objective function penalises under-design more than over-design. This is seen as a desirable property when

calibrating a design standard.

The steps in the calibration process are described in more detail in the following sections of the paper. Some testing and checking of the design standard is carried out after an optimum safety factor has been determined.

3 SCOPE OF DESIGN STANDARD

The design code is intended to be applicable to positioning systems for most types of offshore platforms all over the world, in water depths down to about 2000m. Slack (catenary type), semi-taut and taut mooring systems are included, with chain and steel wire rope line segments. The standard also include synthetic fibre mooring line, but these components are excluded from the present calibration. Thruster assisted systems are included, but dynamic positioning (without any mooring lines) is not covered. Mobile and permanent platforms for drilling, production, storage, maintenance and accommodation are included. Postioning of platform types such as semisubmersibles and turret-moored ships, as well as slack moored loading buoys are covered, while tension leg platforms are excluded. The design standard covers the evaluation of environmental loads on the system, resulting platform motions and mooring line tensions, and the dimensioning of the mooring line components.

3.1 Test set

Six different application examples were selected for the test set. They comprise a turret-moored ship and a semisubmersible, each moored at three different water depths; i.e. 70 m, 350 m and 2000 m for the ship and 70 m, 350 m and 1000 m for the semisubmersible. The main particulars of the ship and the semisubmersible are given in Table 1. A spar platform was not included in the test set, but some guidance concerning the fatigue effects of vortex-induced motions, which have been encountered with this platform type, is included in the most recent version of DNV's standard[4].

ITEM	Ship	Semisubmersible
Length (m)	215	121
Breadth o.a. (m)	42	95.3
Draught (m)	16	21
Distance midship-turret (m)	90	-
Displacement (tonnes)	120 000	52 500
Number of Columns	-	4
Column cross-section (m)	-	16.6 × 16.6
Number of pontoons	-	4
Pontoon breadth × height (m)	-	16.6 × 8.4

Table 1 Main parameters of platforms in the test set.

The ship is equipped with 8 mooring lines evenly spread around the compass directions. The semisubmersible has 12 mooring lines in clusters of 3 lines at each corner, where the angles between the lines in a cluster are 5 degrees. Separate mooring systems were specified for the ship and the semisubmersible at the different water depths. Realistic combinations of wire and chain segments were used, and dimensioned according to the ultimate limit state of

the existing design standard. All lines within each system are identical. A buoy was included in the lines for the case in 2000 m water depth.

Environmental conditions representative of the Norwegian Sea, from Haltenbanken, are applied, including wind, wave and current effects. The actual empirical frequencies of the various compass directions are used, such that the fatigue damage varies between the lines of a mooring system. Alternative environmental conditions from the Gulf of Mexico were also considered in the calibration of the ultimate and accidental limit states, but this was not considered necessary for the fatigue limit state, because of the close correspondence between the design and reliability analyses for fatigue.

4 RELIABILITY ANALYSIS

The reliability analysis applied in the present calibration is based on the model developed in the PROMOOR joint industry project[6][7]. The calibration is intended to provide a good basis for the design of mooring line segments made of chain or steel wire rope. Thus, the main focus of the work is on these types of components, on the random modelling of their fatigue properties, and on the effect of many components of these types. The formulation of the reliability analysis is briefly presented below, together with a specification of the probability distributions of the random variables that are involved.

4.1 Failure of a single component

A mooring line may be assembled from a large number of different components, of various types, such as chain links, connecting links, steel wire rope segments, synthetic rope segments and rope terminations. Fatigue failure is conceivable in any of these components. The possibility of failure in each individual component may be assessed on the basis of the Miner-Palmgren hypothesis. Under this hypothesis, the fatigue damage experienced by a single component is expressed by

$$d = n_0 \int_0^\infty \frac{f_S(s)}{n_C(s)}\, ds \qquad \textbf{(1)}$$

where n_0 is the total number of stress cycles encountered by the component, s represents the peak-to-trough range of a stress cycle, $f_S(s)$ is the probability density function of the stress ranges, and $n_C(s)$ is the number of stress cycles at constant stress range s required to induce fatigue failure in the component. This fatigue property of the component is usually determined experimentally and expressed by a function of the type

$$n_C(s) = a \cdot s^{-m} \qquad \textbf{(2)}$$

where a is the intercept parameter and m is the slope parameter of the S-N curve in logarithmic form; c.f. section 4.4. Substitution of equation (2) into equation (1) gives

$$d = \frac{n_0}{a} \int_0^\infty s^m \, f_S(s)\, ds \qquad \textbf{(3)}$$

indicating that the fatigue damage is proportional to the expected value of the stress ranges raised to the power *m*; i.e. $E\left[S^m\right]$. In practice, it is convenient to first compute the contribution to the fatigue damage from a stationary environmental state, and subsequently integrate over the domain of environmental states to obtain the total fatigue damage

$$d = \frac{t_D}{a} \int_{\boldsymbol{\Psi}} \nu(\boldsymbol{\psi})\, E\left[S^m(\boldsymbol{\psi})\right] f_{\boldsymbol{\Psi}}(\boldsymbol{\psi})\, d\boldsymbol{\psi} \tag{4}$$

where t_D is the service life duration, $\boldsymbol{\Psi}$ is the environmental state vector, $\nu(\boldsymbol{\psi})$ is the mean up-crossing rate of the stress process through the mean value, and $f_{\boldsymbol{\Psi}}(\boldsymbol{\psi})$ is the joint probability density function of the environmental variables. The environmental state vector includes components describing the heading angles, as well as wind, wave, and current conditions. Both wave-frequency and low-frequency contributions to the stress ranges are included. The dual narrow-banded approach is used to compute the expected value of the stress ranges raised to the power *m* in the individual environmental states. This approach has been developed by Jiao[8], and applied to mooring line fatigue by Lie and Fylling[9].

The fatigue damage expressed by equation (4) is a deterministic quantity as it stands. Random variables are involved in the environmental states and in the stress process, but the integration in equation (4) effectively provides a deterministic expected value as the result. In practice, the fatigue damage is known to be associated with considerable uncertainty, implying that it should be treated as a random variable. This characteristic is built into the present model by including the uncertainty present in the various quantities involved in equation (4). The following model uncertainties are included:

Q_1 for the computed low-frequency motion of the upper terminal point on the platform,

Q_2 for the computed wave-frequency motion of the upper terminal point,

Q_3 for the mooring line response model for quasi-static tension, arising from mean offset and low-frequency motions of the platform,

Q_4 for the mooring line response model for dynamic tension, arising from wave-frequency motion of the platform,

Q_5 for the cycle-counting algorithm used to combine the low-frequency and wave-frequency stress components,

Q_6 for the Miner-Palmgren hypothesis for the combination of fatigue damage due to stress cycles of a stochastic process, based on results of tests at constant frequencies and amplitudes, and excluding explicit consideration of the mean stress,

These model uncertainties may all be conveniently collected in the random vector $\mathbf{Q}$. This random vector only includes components that apply to all physical components of a mooring line segment. Hence, it may be referred to as a global variable.

In addition, there is an inherent variability between the fatigue strength of different mooring line components. This uncertainty may be modelled by treating the intercept parameter of the S-N curve as a random variable, and quantifying its variability from the experimental test data, as discussed in section 4.4. This variability may be split into two parts:

Q_7 the global uncertainty in the intercept parameter for a type of mooring line components applied in a specific mooring line,

L the local variability in the intercept parameter between components of the same type, within a specific mooring line.

The first of these two items takes on the same value for all components of a single type, within a specific mooring line, hence it is included in the vector $\mathbf{Q}$. The second varies randomly between components of the same type and manufacture, within a specific mooring line, and the random variable L is introduced to represent this trait.

Either one or both the parameters of the S-N curve could be treated as random variables. In the present case only the intercept-parameter *a* is treated randomly, such that

$$\log(a)=q_7+l \tag{5}$$

The effects of these random variables may now be indicated by rewriting equation (4) as

$$d(l,\mathbf{q})=\frac{t_D}{a(l,q_7)}\int_{\Psi}\nu(\boldsymbol{\psi},\mathbf{q})\,E\left[S^m(\boldsymbol{\psi},\mathbf{q})\right]\,f_{\boldsymbol{\Psi}}(\boldsymbol{\psi})\,d\boldsymbol{\psi} \tag{6}$$

where the model uncertainty factors $q_1,...,q_5$ are associated with the corresponding variables in the computation of stress ranges and mean up-crossing rate.

The probability of failure of a single component may be expressed by

$$P_{f1}=P\left[D(L,\mathbf{Q})>Q_6\right] \tag{7}$$

where the Miner-Palmgren uncertainty Q_6 would typically taken as unity in a deterministic analysis. The usual convention is applied, of using upper case symbols for the random variables themselves, and the corresponding lower case symbols for realisations of these random variables.

4.2 Failure of Many Components of the Same Type

Consider $i=1,2,...,I$ mooring line components of a particular type; e.g. chain links of a specific type, dimension and manufacture. The same stress ranges are assumed to apply to all components of the same type in a single mooring line, for the purpose of this fatigue analysis. This is a reasonably good approximation, which considerably simplifies the analysis. The fatigue damage function for each component is simply obtained from equation (6), by attaching an index *i*, for the component number, to the only variable that varies between components of the same type, namely *l*, the local variability of the *a*-parameter of the S-N curve,

$$d_i(l_i,\mathbf{q})=\frac{t_D}{a(l_i,q_7)}\int_{\boldsymbol{\Psi}}\nu(\boldsymbol{\psi},\mathbf{q})\,E\left[S^m(\boldsymbol{\psi},\mathbf{q})\right]f_{\boldsymbol{\Psi}}(\boldsymbol{\psi})\,d\boldsymbol{\psi}\,,\quad i=1,2,...,I \tag{8}$$

The probability of failure of the part of the line containing these components is expressed by the complement of the probability that no component shall fail; i.e. by the intersection of the survival events for all components

$$P_{fI} = 1 - P\left[\bigcap_{i=1,\ldots,I} D_i(L_i, \mathbf{Q}) \le Q_6\right] \tag{9}$$

The survival events for the individual components are not stochastically independent. They are dependent on the random vector $\mathbf{Q}$. However, by considering the probability of failure conditional on this random vector, independent component events are obtained

$$P_{fI|\mathbf{Q}}(\mathbf{q}) = 1 - P\left[\bigcap_{i=1,\ldots,I} D_i(L_i, \mathbf{q}) \le q_6\right] \tag{10}$$

The multiplication rule may now be applied to obtain

$$\begin{aligned} P_{fI|\mathbf{Q}}(\mathbf{q}) &= 1 - \prod_{i=1,\ldots,I} P\left[D_i(L_i, \mathbf{q}) \le q_6\right] \\ &= 1 - \left[F_{D_i|\mathbf{Q}}(q_6|\mathbf{q})\right]^I \end{aligned} \tag{11}$$

where $F_{D_i|\mathbf{Q}}(d|\mathbf{q})$ is the conditional probability distribution of the damage for an individual component of this type, which can conveniently be computed using the PROBAN program[10]. The problem formulation has been arranged to make the component-wise uncertainty L_i independent and identically distributed between components of the same type, so that the multiplication rule can be applied to obtain equation (11).

The marginal probability of failure for these components is obtained using the theorem of total probability

$$P_{fI} = \int_{\mathbf{Q}} P_{fI|\mathbf{Q}}(q)\, f_{\mathbf{Q}}(\mathbf{q})\, d\mathbf{q} \tag{12}$$

where $f_{\mathbf{Q}}(\mathbf{q})$ is the probability density function for the global uncertainty vector $\mathbf{Q}$. This is the accumulated probability of failure at any time in the design life t_D. The probability of failure prior to the last year is obtained by using $(t_D - 1)$ in the expressions above (provided t_D is in units of years). The marginal probability of failure in the last year is the difference between these two probabilities. In principal, it seems more correct to consider the conditional probability of failure in the last year for the purpose of initial design, by assuming that a fatigue failure does not occur prior to the last year. However, there is negligible difference between the marginal and conditional probabilities of failure in the final year, when the accumulated probability of failure is small. (The difference can become significant when the accumulated probability is not small, but this would be inappropriate in design.)

This completes the probabilistic formulation of the fatigue limit state for a segment of a mooring line. An extension to several segments of different types is straight forward, but seldom necessary, because one type of component usually tends to dominate the probability of failure of a line. To compute failure probabilities, it is necessary to specify the distributions of the random variables, and to calculate the spectral moments of the stress

ranges, in a representative set of environmental states. The MIMOSA program[11] is used to calculate the line tensions in the present case.

4.3 Failure of two lines

Fatigue failure of a single mooring line is often viewed as an event with minor consequences, beyond the cost of repairing or replacing the failed line. After all, design with respect to the accidental limit state ensures that mooring systems have a certain amount of redundancy. However, fatigue failure of a second line, before the first failure has been rectified, may be much more serious and this possibility needs to be considered.

It is common practice to employ similar mooring line components in all the mooring lines attached to a single platform. The main body of each line is composed of a large number of components (chain links or segments of wire rope) of the same type, or of a few different types. Although there is likely to be considerable variation in the fatigue capacity of the individual components, the fatigue capacity of each line will be governed by the fatigue capacity of the weakest component in each line. The process of selecting the weakest component from a large number of similar components tends to reduce the final variability considerably; i.e. mooring lines constructed from many identical components tend to have very nearly the same fatigue capacity.

When mooring lines are equally spaced around a platform, then the usual variation of the environmental loading around the platform will tend to ensure that one or two lines experience a higher fatigue load than the other lines. The spacing between the lines tends to govern the difference in the fatigue loads. If the lines are widely spaced, then there is likely to be appreciable difference between the highest fatigue load, and the fatigue load in an adjacent line. If two lines are closely spaced, then they will tend to experience very nearly the same fatigue load.

If a line contains a fatigue crack that has grown to a significant size, then fatigue failure is most likely to occur in a moderate or severe storm, when the tension in the line is sufficient to overcome the residual strength of the line. If an adjacent line has nearly the same fatigue strength, and has experienced nearly the same fatigue load, then it may well fail in the same storm. This scenario is exacerbated by the increase in tension due to the initial failure. Such a situation should, in many cases, be considered to have substantial consequences, because further damage may then be very likely; e.g.

- collision with a platform that is within reach after two lines have failed, or
- fracture of risers leading to pollution and/or fire/explosion, or
- complete mooring system failure, and risk of collision with other platforms.

Note that the fatigue failures may well occur in a moderate storm which is not sufficiently severe to require shut down of normal drilling or production operations.

This qualitative discussion clearly needs to be followed up by some quantitative analysis. The S-N type fatigue analysis that is employed here is not ideal for this purpose, because it implies a uniform rate of fatigue damage, and does not model the final rupture event in any detail. Fracture mechanics models are better suited. However, the S-N analysis can be bent to this task by jointly considering initial fatigue failure of one line in the final year of the design life, and subsequent failure of a second line within one month of the initial failure.

This one month interval is intended to roughly represent the incremental fatigue damage, and rupture possibility, that would be accumulated in the second line during the same storm.

The probabilistic formulation of this two-line failure event is most conveniently written in terms of the random time to line failure T_f, rather than the maximum accumulated damage in any component of the line D that is considered above. This change is simply accomplished using, in principal,

$$t_f(\mathbf{q}) = \frac{q_6 \cdot t_D}{d(\mathbf{q})} \tag{13}$$

where the extreme minimum distribution of the intercept parameter a amongst the components of the line segment is applied in computing the damage rate. The combined event is composed of the underlying events

- failure of line A in the design life $T_{fA} < t_D$
- survival of line A up to the last year of the design life $T_{fA} > t_D - 1$
- failure of adjacent line B within one month after failure of line A $T_{fB} - T_{fA} < 1/12$
- survival of line B up to the last year of the design life $T_{fB} > t_D - 1$

Hence, the combined probability may be written as

$$P\left[\left(T_{fA} < t_D \bigcap T_{fB} - T_{fA} < \frac{1}{12}\right) \middle| \left(T_{fA} > t_D - 1 \bigcap T_{fB} > t_D - 1\right)\right] \tag{14}$$

There is an inaccuracy in this formulation of the combined probability, because it includes the possibility of failure of line B prior to line A, during the final year. However, the effect of this inaccuracy should be relatively small in the analysis, because line B is modeled as the line with the lesser fatigue loading.

4.4 Fatigue capacity

In order to obtain a consistent calibration of safety factors for fatigue, it is important to have consistency between the fatigue curves applied in the reliability analysis, and the corresponding curves applied in the design analysis. Fatigue testing is both expensive and time consuming, and only limited amounts of data are available. Generally there are a large number of physical effects that may affect the fatigue capacity, and there has been a tendency for investigators to address too many variables from too few tests, thus diluting the overall value of the test results [12]. In addition, the test procedures and results are often not fully documented, which makes misinterpretation of test data possible.

The present work tries to combine established design practice with additional knowledge gained from analysis of test results. In particular, statistical analysis has been performed on fatigue test data for mooring chain, provided to the project by Scana Ramnäs[13] (32 tests) and by Vicinay Cadenas (19 tests). Additionally, 14 tests from an extensive joint industry study on studless chain fatigue[14] were also considered. Finally, results of available chain tests[12] have also been used.

No new data for steel wire rope have been analysed in the present work. A review of test data for both chain and steel wire rope was performed and presented in [6], based on work carried out at Transport Research Laboratory[15]. The results from that study are considered in the present work.

The basic equation for the S-N curve is given in equation (2). Nominal stresses are used, obtained by dividing the line tension by the nominal cross-sectional area of the chain ($\pi / 2 \times \text{diameter}^2$) or the wire rope ($\pi / 4 \times \text{diameter}^2$). The stress basis is preferred to the relative tension basis applied to chain in API RP 2 SK[16], because the normalisation with respect to the breaking strength of ORQ type chain is arbitrary and involves a term in the cube of the chain diameter. This term is presumably relevant with respect to nonlinear link behaviour at the very high stresses required to break a link, but not for linear link behaviour at the low stresses involved in fatigue. This approach might be criticised with respect to wire rope, because the nominal area is different from the actual steel cross-sectional area. However, this criticism can largely be avoided by treating different rope constructions separately.

Equation (2) is written in a logarithmic from for the purpose of fitting the test data:

$$\log(n) = \log(a) - m \cdot \log(s) \qquad \textbf{(15)}$$

The fatigue test data have been analysed, and $\log(a)$ and m have been computed by linear regression analysis. The standard deviation of $\log(a)$ is computed for m fixed, and represents the uncertainty in the S-N curve. An approach[18] to handle run-outs (components which did not fail during a limited test duration) was applied in some of the exploratory analyses, but it had a relatively small effect on the fitted parameters, and was not used on the results shown here.

The present calibration work for fatigue focuses on the main body of mooring lines. Only tension fatigue is considered. Fatigue properties for line terminations and connecting links are not discussed further here. Recent results for additional stresses in chain links on a fairlead may be found in ref.[17].

The statistical analysis showed that the uncertainty comprising all tests is greater than for individual sub-sets. The uncertainty has been divided into a local and a global uncertainty in the intercept parameter to reflect this behaviour. The global uncertainty models the uncertainty relative to the generic mean S-N curve, for a certain type of mooring line components applied in a specific mooring line, whereas the local uncertainty reflects the variability between components of the same type within that mooring line. The test results give some support for an approximately equal split between local and global uncertainty.

A summary of the fatigue parameters used in the reliability analysis and for the design analysis is included in Table 2. It was found necessary and sufficient to distinguish between results for stud-link and studless chain, and between six-strand and spiral-strand rope.

	No of tests	Fatigue curve parameters				PROBAN input	
		Design a_d	Mean a	m	Std.dev. log(a)	Mean log(a)	Variance log(a)
CHAIN							
Stud-link	174	$1.2 \cdot 10^{11}$	$3.52 \cdot 10^{11}$	3.0	0.26	11.55	0.0576
Studless	66	$6.0 \cdot 10^{10}$	$1.80 \cdot 10^{11}$	3.0	0.14	11.26	0.0576
STEEL WIRE ROPE							
Six strand	96	$3.4 \cdot 10^{14}$	$1.04 \cdot 10^{15}$	4.02	0.29	15.02	0.0576
Spiral strand	16	$1.7 \cdot 10^{17}$	$4.99 \cdot 10^{17}$	4.84	0.20	17.70	0.0576

Table 2 S-N fatigue parameters for the reliability and design analysis.

Standard procedure is to take the design curve at 2 standard deviations below the mean curve. This procedure is followed here, but some judgement is applied to the evaluated standard deviations. There is a fair amount of variation in most cases, except for studless chain which is heavily dominated by one set of experiments, from one laboratory, for 76 mm diameter chain. This may possibly be the reason why a much lower residual variability is obtained for studless chain in Table 2. It does not seem prudent to take full advantage of this result when establishing a generic design curve, until it has been better confirmed for a wider set of conditions. Instead it is proposed to apply a weighted mean value of 0.24 for the standard deviation in *log(a)* to all 4 component types included here. Thus the design values in Table 2 are obtained as:

$$\log(a_d) = \log(a) - 2 \times 0.24 \qquad \textbf{(16)}$$

The regression results were generally not very sensitive to the m value. For chain the value of 3 represents a reasonable compromise for the various sub-sets, including salt water tests. The actual value obtained in the regression analysis is used for steel wire rope.

Results from chain tests[12],[13],[14] were used to quantify the effect of salt water on chain endurance as compared to tests in air. A reduction factor of 2 on fatigue life was found for stud-link chain. This factor is low compared to the factor of 3 incorporated in ref.[19]. On the other hand, a reduction factor of 5 was found for studless chain. The difference in these results for the two types of chain links is puzzling.

The thickness effect was also investigated for chain links. This effect was found to be relatively small compared with other welded structures, and some slightly conflicting results were obtained for R3 and R4 chain. The application of a thickness correction was therefore rejected.

A comparison of the API recommended practice[16] with the present results was carried out. The difference for stud-link chain is relatively small. For steel wire rope the API curve is somewhat more conservative, especially for six-strand rope. The effect of mean load, as accounted for in the API rules, has not been included here since this could not be justified on the basis of the test results that were considered.

4.5 Random variables

The distributions of the random variables that are applied in the reliability analysis are summarised in Table 3. The model uncertainties on the line tension calculation are as used in

ref.[7], and based on comparisons of calculations by MIMOSA[11] with model tests and alternative calculations. The uncertainty in the cycle-counting algorithm is based on the comparison of the dual narrow band algorithm with rainflow counting by Lie and Fylling[9].

Wirsching and Chen[21] have collected information on the uncertainty in the Miner-Palmgren hypothesis. They cite a number of investigations with median damage at failure ranging from 0.69 to 1.15 and coefficient of variation (CoV) from 0.19 to 0.67. They have applied a log-normal distribution with median 1.0 and CoV 0.30 in their example for TLP design criteria[20]. This corresponds to a mean value of 1.04 and standard deviation of 0.31, as specified here.

Variable	**Symbol**	**Distribution**	**Mean value**	**Std.dev.**
Uncertainty in LF motion	Q_1	Normal	1.0	0.1
Uncertainty in WF motion	Q_2	Included in Q_4	-	-
Uncertainty in QS tension calculation	Q_3	Normal	1.0	0.02
Uncertainty in dynamic tension calculation	Q_4	Normal	0.9	0.1
Uncertainty in cycle-counting algorithm	Q_5	Normal	1.0	0.1
Uncertainty in Miner-Palmgren hypothesis	Q_6	Log-normal	1.04	0.31
Global uncertainty in log(a) parameter	Q_7	Normal	see Table 2	$\sqrt{k_g \cdot Var(\log a)}$ (base case k_g=0.5)
Local uncertainty in log(a) parameter	L	Normal	0.0	$\sqrt{(1-k_g) \cdot Var(\log a)}$
Designer uncertainty		Normal	1.0	0.04

Table 3 Distributions of random variables.

The overall variance in $\log(a)$ is based on the analysis of fatigue test data in section 4.4. This is split into a global and a local part using the factor k_g. This factor is set to 0.5 for the base case analysis. This seems to be a reasonable estimate, but there is little information available to support this value. Variation of this factor can be used to investigate the effect of assuming that nearly all the variability is global ($k_g = 0.9$), or nearly all the variability is local ($k_g = 0.1$).

Test case	Number of components considered
Ship in 70 m depth	765
Ship in 350 m depth	1744
Ship in 2000 m depth	1223
Semisubmersible in 70 m depth	765
Semisubmersible in 350 m depth	2216
Semisubmersible in 1000 m depth	1357

Table 4 Number of chain link or wire components considered in each mooring line.

A designer uncertainty is included. This is not normally relevant to a reliability analysis. It is included to simulate the effect of taking account of design calculations from different

designers in the calibration process, and is applied as a factor on the line diameter.

The numbers of components taken into account in the reliability analysis are given in Table 4.

5 DESIGN ANALYSIS

The design format of the fatigue limit state is written as

$$1 - \gamma \cdot d_C \geq 0 \qquad \textbf{(1)}$$

where γ is the fatigue safety factor and d_C is the characteristic fatigue damage. The characteristic fatigue damage in a mooring line segment is computed as indicated by equation (4), using the design value of the intercept parameter a_D from Table 2. The integration over environmental states is carried out as a discrete summation, and assumed to be finely enough discretised as to avoid any significant error. The dual narrow-banded cycle counting algorithm is applied, or some other algorithm of comparable accuracy (e.g. rainflow counting), or a more conservative algorithm (e.g. the combined spectrum method). No explicit account is taken of the number of components in the line segment.

A damage factor d_f between two adjacent lines is defined as the ratio of the lesser characteristic fatigue damage to the greater damage of these two lines. This damage factor is introduced to evaluate the possibility of two line failures.

6 TARGET LEVEL

Insufficient experience with the fatigue design of mooring lines was deemed to be available, to provide a suitable basis for the target reliability. Hence, comparison with the safety levels of "transferable" structures was chosen as the method[5] to derive this target. Fatigue design requirements set by the Norwegian Petroleum Directorate[22] and widely applied in the design of jacket platforms were chosen. A similar reliability analysis to the present analysis was applied, based on Sigurdsson and Cramer's work[23]. The results are shown in Table 5. Both these cases apply to jacket welds that are in the splash zone or that are inaccessible. The jacket safety factor of 10 is classified for "substantial consequences," while the factor of 3 is for "without substantial consequences."

Jacket fatigue design factor γ_f	Accumulated failure probability	Failure probability in last year	Selected annual target values
3	6.6×10^{-3}	1.1×10^{-3}	1.0×10^{-3}
10	2.9×10^{-5}	7.2×10^{-6}	1.0×10^{-5}

Table 5 Computed probabilities of failure for the fatigue limit state applied to welded joints of jacket platforms. S-N curve parameters for joint class F2[19], with design life $t_d = 20$.

7 CALIBRATION RESULTS

Calibration results for a single line are shown in Figure 2. For the base case, with global variability factor $k_g = 0.5$, the target level "without substantial consequences" is achieved

with a fatigue safety factor of 5. It may be seen that the value of the safety factor is strongly dependent on the target level, and on the global variability factor. With mainly global variability $k_g = 0.9$, the safety factor corresponds to the original factor for a weld in a jacket platform; i.e. a safety factor of 3.

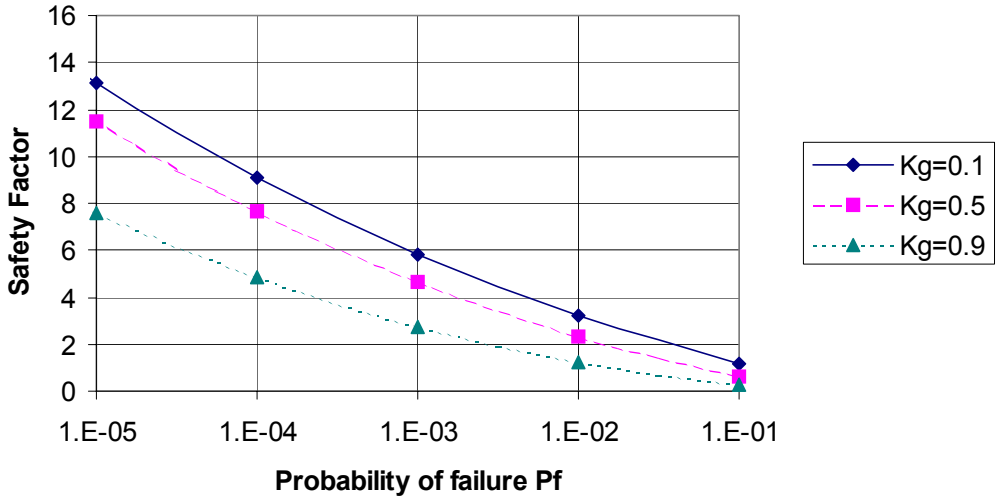

Figure 2 Safety factor as a function of target annual probability level, using S-N data with standard deviation of $\log(a) = 0.24$, $m = 3$, for various global variability factors $k_g = 0.1, 0.5, 0.9$. A single line is considered.

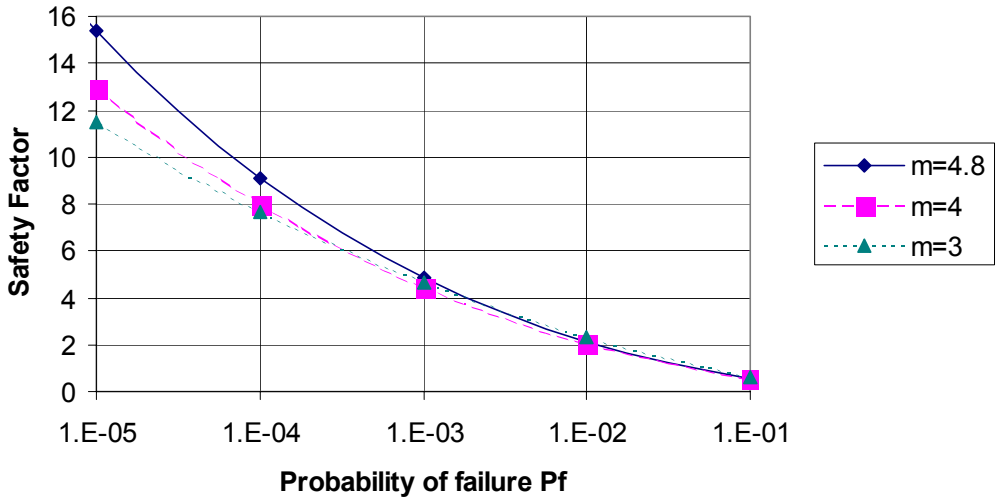

Figure 3 Safety factor as a function of target annual probability level, using S-N data with standard deviation of $\log(a) = 0.24$, $k_g = 0.5$, for various values of slope parameter *m*. A single line is considered.

Figure 3 indicates that the safety factor is only weakly dependent on the slope parameter *m*, at this consequence level. Hence, the same safety factor can be applied to chain links and

both types of steel wire rope components.

Calibration results for the two line failure event are shown in Figure 4. This case is taken to have "substantial consequences," such that a target probability of failure of 10^{-5} is appropriate. Considering the base case, with global variability factor $k_g = 0.5$, it may be seen that the safety factor of 5 obtained from the single line evaluation corresponds to the two line evaluation at a fatigue damage factor of 0.8 between adjacent lines. A higher safety factor is required when the damage factor between adjacent lines is higher. This safety factor can be well approximated by linear interpolation as

$$\gamma = 5 + 3(d_f - 0.8)/0.2, \quad d_f > 0.8 \qquad \textbf{(1)}$$

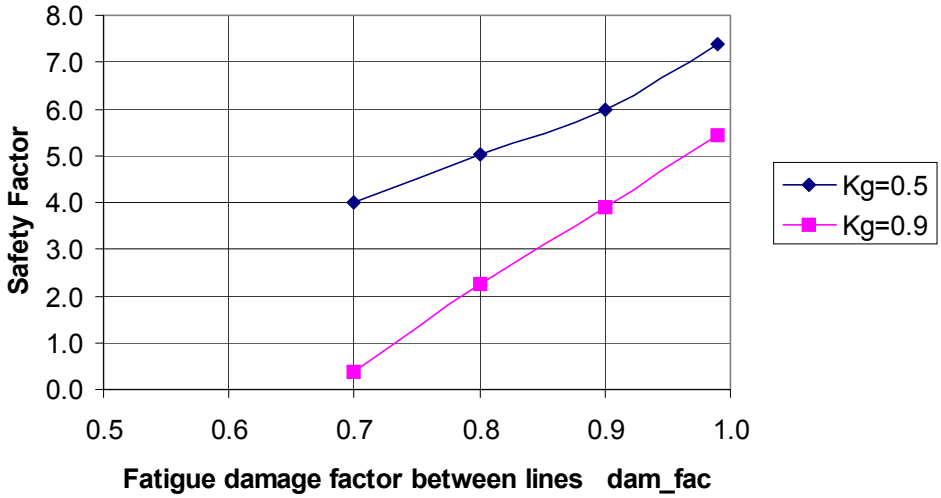

Figure 4 Safety factor as a function of fatigue damage factor between 2 lines, with target annual probability level 10^{-5} and various values of global variability factor.

Further details of the reliability analyses and calibration are include in ref.[3].

8 CONCLUSIONS

The calibration of a fatigue design code for mooring lines has been carried out on the basis of structural reliability analysis. The analysis has revealed a potential for fatigue failure of two adjacent mooring lines in the same storm. The fatigue reliability analysis has been extended to quantify this risk in an approximate way, and these results have been utilised in the calibration.

It is recommended to develop a fracture mechanics model to analyse the potential for two line failures in the same storm more accurately. Additional data from chain link fatigue tests would also be desirable, to establish the S-N curves with more confidence, and to better quantify the difference between global and local variability of the fatigue capacity.

9 ACKNOWLEDGEMENTS

The authors gratefully acknowledge the support of the participants in the DEEPMOOR joint industry project: Advanced Production and Loading, Bridon International, Conoco Norge, Det Norske Veritas, the Health and Safety Executive, Lloyd's Register, Norsk Hydro, Norske Shell, the Norwegian Maritime Directorate, the Norwegian Shipowners' Association, the Royal Norwegian Research Council, Scana Ramnäs, Statoil, and Vicinay Cadenas. The project has been carried out in cooperation between Det Norske Veritas and Marintek. Vibeke Moe and Walter Lian of Marintek carried out the line tension calculations. The material presented herein should not necessarily be taken to represent the views of any of these companies.

REFERENCES

[1] Hørte, T., Lie, H., Mathisen, J., (1998), "Calibration of an Ultimate Limit State for Mooring Lines", 17th Offshore Mechanics and Arctic Engng. Conf., OMAE-1457, Lisbon.

[2] Mathisen, J., Larsen, K., Hørte, T., Lie, H., (1998), "Calibration of a Progressive Collapse Limit State for Mooring Lines", 17the Offshore Mechanics and Arctic Engng. Conf., OMAE-1458, Lisbon.

[3] Mathisen, J., Hørte, T., Moe, V., Lian, W., (1999), "DEEPMOOR – Design Methods for Deep Water Mooring Systems, Calibration of a Fatigue Limit State," Det Norske Veritas, Report no. 98-3110, rev.no, 03, Høvik.

[4] Det Norske Veritas, (2004), "Offshore Standard DNV-OS-E301 Position Mooring," Høvik.

[5] Det Norske Veritas, (1992), "Structural Reliability Analysis of Marine Structures," Classification Note No. 30.6, Høvik.

[6] Mathisen, J., Fylling, I., Hørte, T., (1995), "An Approach to Reliability Analysis of Mooring Lines with Respect to the Fatigue Limit State," Det Norske Veritas, report no. 95-3208, Høvik.

[7] Larsen, K., Mathisen, J., (1996), "Reliability-Based Fatigue Analysis of Mooring Lines," 15th Int. Conf. Offshore Mechanics and Artic Engineering, paper no.96-1343, ASME, Florence.

[8] Jiao, G., (1989), "Reliability Analysis of Crack Growth under Random Loading Considering Model Updating," pp157, Div. Marine Structures, Norwegian Institute of Technology, MTA report 1989:68 (thesis), Trondheim.

[9] Lie, H., Fylling, I.J., (1994), "Evaluation of Methods for Fatigue Analysis of Offshore Mooring Lines", 10th Offshore South East Asia Conf. and Exhibition, OSEA-94007, Singapore.

[10] DNV, (1996), "SESAM User's Manual: PROBAN, General Purpose Probabilistic Analysis Program," report no. 92-7049/Rev.1, Det Norske Veritas, Høvik.

[11] Mo, K., Lie, H., (1990), "User's Documentation MIMOSA-2, version 2", Marintek, Report No. 519616.00.01, Trondheim.

[12] Casey, N.F., (1996), "A Review of Available Laboratory Test Data on Chain for Mooring Applications," NEL report no. 57/95, National Engineering Laboratory,

Glasgow.
[13] Öberg, H., (1995), “Fatigue Testing of Anchor Chains,” report no. 95-03-14, Dept. Solid Mechanics, Kungl Tekniska Högskolan, Stockholm.
[14] Noble Denton & Associates, Inc., (2002), "Corrosion Fatigue Testing of 76mm Grade R3 & R4 Studless Mooring Chain", Report no. H5787/NDAI/MJW, Rev.0, Houston.
[15] Cuninghame, J.R., (1993), “Review of Tension-Tension Fatigue Performance of Wire Ropes,” report no. PR/BR/23/93, Transport Research Laboratory, (Confidential).
[16] API, (1997), “Recommended Practice for Design and Analysis of Stationkeeping Systems for Floating Structures,” API RP 2SK, American Petroleum Institute, Washington D.C.
[17] Vargas, P.M., Hsu, T.-M., Lee, W.K., (2004), "Stress Concentration Factors for Stud-Less Mooring Chain Links in Fairleads", 23rd Int. Conf. Offshore Mechanics & Arctic Engng., OMAE2004-51376, ASME, Vancouver.
[18] Bratfos, H.A., Cramer, W., Svensson, T., (1997), "Statistical Evaluation of Fatigue Data with Run-outs", Det Norske Veritas, Report no. 97-1220, Høvik.
[19] Det Norske Veritas, (2001), “Fatigue Strength Analysis of Offshore Steel Structures,” Recommended Practice RP-C203, Høvik.
[20] Wirsching, P. H. & Chen, Y.-N., (1987), “Fatigue Design Criteria for TLP Tendons”. ASCE J. Struct. Div., 113 (7) 1398-414.
[21] Wirsching, P. H. & Chen, Y.-N., (1988), “Considerations of Probability-Based Fatigue Design for Marine Structures”, Marine Structures, Design, Construction & Safety, Vol. 1, ISBN: 0951-8339.
[22] NPD, (1998), “Acts, regulations and provisions for the petroleum activities, Vol.2, Regulations relating to loadbearing structures in the petroleum activities,” Norwegian Petroleum Directorate, Stavanger.
[23] Sigurdsson, G., Cramer, E., (1996), “Guideline for Offshore Structural Reliability Analysis: Examples for Jackets,” Det Norske Veritas, report no. 95-3204, Høvik.